Chapter 29

In Vitro Reconstitution of Kinesin-Based, Axonal mRNA Transport

Julia Grawenhoff, Sebastian Baumann, and Sebastian P. Maurer

Abstract

Motor protein-driven transport of mRNAs on microtubules and their local translation underlie important neuronal functions such as development, growth cone steering, and synaptic plasticity. While there is abundant data on how membrane-bound cargoes such as vesicles, endosomes, or mitochondria are coupled to motor proteins, surprisingly little is known on the direct interactions of RNA–protein complexes and kinesins or dynein. Provided the potential building blocks are identified, in vitro reconstitutions coupled to Total Internal Reflection Microscopy (TIRF-M) are a powerful and highly sensitive tool to understand how single molecules dynamically interact to assemble into functional complexes. Here we describe how we assemble TIRF-M imaging chambers suitable for the imaging of single protein–RNA complexes. We give advice on optimal sample preparation procedures and explain how a minimal axonal mRNA transport complex can be assembled in vitro. As these assays work at picomolar-range concentrations of proteins and RNAs, they allow the investigation of molecules that cannot be obtained at high concentrations, such as many large or disordered proteins. This now opens the possibility to study how RNA-binding proteins (RBPs), RNAs, and microtubule-associated proteins act together in real-time at single-molecule sensitivity to create cytoplasmic mRNA distributions.

Key words Cytoplasmic mRNA localization, Axonal transport, Kinesins, In vitro reconstitution, Single-molecule imaging

1 Introduction

Cells spatially regulate gene expression through the active, microtubule-dependent localization and local translation of mRNAs. This is of fundamental importance for diverse processes requiring the configuration of cellular domains with distinct protein sets [1–3]. Mammalian neurons are a fascinating, well-studied model system demonstrating the importance of mRNA localization. Neurons require localized translation for development [4, 5], axonal growth cone steering [6, 7], synaptic plasticity [8], and

Julia Grawenhoff and Sebastian Baumann contributed equally to this work.

Alessio Vagnoni (ed.), *Axonal Transport: Methods and Protocols*,
Methods in Molecular Biology, vol. 2431, https://doi.org/10.1007/978-1-0716-1990-2_29,

long-term memory formation [9]. To generate mRNA distributions, bidirectional microtubule (MT)-motor-based transport machines "read" localization information that is encoded in mRNA 3′UTRs. This is mediated by RBPs that bind these localization signals and potentially control mRNA–motor coupling through largely unknown mechanisms. While discoveries of biological or disease-related processes depending on mRNA transport increase [10, 11], we just begin to understand how kinesins, dynein, and mRNA cargo adaptors assemble to distribute mRNAs in neurons or mammals in general. A thorough mechanistic understanding of this process, however, is key to disentangle and potentially control the molecular causes of neurodegenerative disease and viral infections [12, 13] impairing the nervous system or mammalian cells in general. The current lack of understanding might have several causes. First, mRNA transport complexes were widely studied by co-immunoprecipitation approaches [14–17]. While this produced long lists of factors *potentially involved* in mRNA transport, such methods inform about *physical* but not *direct* interactions. Knowledge of the latter, however, is essential to understand the construction principles of mRNA transport complexes. Additionally, RBPs often contain intrinsically disordered regions [18] which tend to aggregate during isolation procedures [19] and capture non-physiological interactors. Second, loss-of-function studies are often hard to interpret; many RBPs are required for splicing, nuclear export, translation regulation, and mRNA transport while motor proteins transport vesicles, proteins, mRNAs, and organelles. Entire deletion of an RBP or motor affects several processes making an analysis of its specific contribution to mRNA transport difficult. Lastly, while omics approaches created a system-level view of mRNA localization and local translation [20, 21], they cannot reveal the biochemical processes that give rise to the system states they report. Recent advances using in vitro reconstitutions shed light on this aspect, revealing the first yeast [22, 23] and *Drosophila* [24] mRNA transport systems. However, as homologs of involved proteins are yet to be identified in mammals, still little was known about the design principles of mammalian mRNA transport complexes.

Separate publications link the microtubule plus-end-tracking protein APC to mRNA localization while others show that APC is transported by the heterotrimeric kinesin-2 KIF3AB and its cargo adaptor KAP3 (KIF3ABKAP3) in axons. These data prompted us to test whether a minimal, reconstituted APC-KIF3ABKAP3 complex is sufficient for selective transport of axonal mRNAs. To this end, we purified recombinant, SNAP-tagged [25] versions of APC as well as KIF3ABKAP3 and obtained fluorescently labeled 3′UTR fragments of the β-actin and β2B-tubulin mRNAs. TIRF-M live imaging of different combinations of these three factors (kinesin, APC, RNAs) in custom-assembled microscopy chambers (Figs. 1

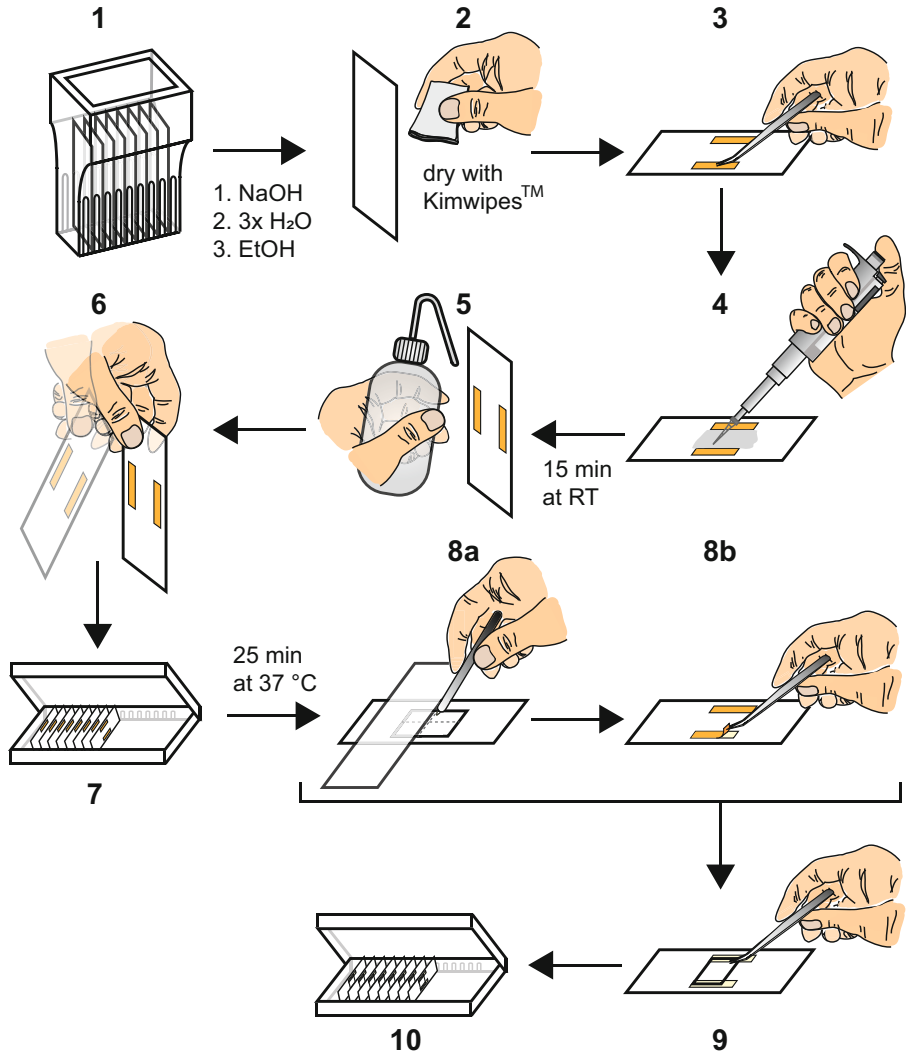

Fig. 1 TIRF-M chamber assembly. Microscopy chambers are prepared as indicated in the individual steps and described in Subheading 3.1. Considering experiment length and that chambers should be freshly made, 1 day of microscopy requires around eight chambers

and 2) allowed us to reveal their dynamic interplay and function (Fig. 3). Using the Fiji plugin Trackmate [26] (Fig. 4), we read out the dynamics (Fig. 5) and the fluorescent intensities of the reconstituted complexes. Subsequent calibration of individual intensities of the used TMR and Alexa647 dyes (Figs. 6 and 7) enables to determine the stoichiometry of reconstituted mRNA transport complexes and subcomplexes. Taken together, this approach demonstrates that the kinesin-2 adaptor KAP3 couples APC-RNA complexes to KIF3AB for processive mRNP transport along microtubules [27]. APC's selectivity of G-rich RNA sequences allows selective transport of both β-actin and β2B-tubulin 3′UTR fragments. While APC was found to be dimeric even at lowest

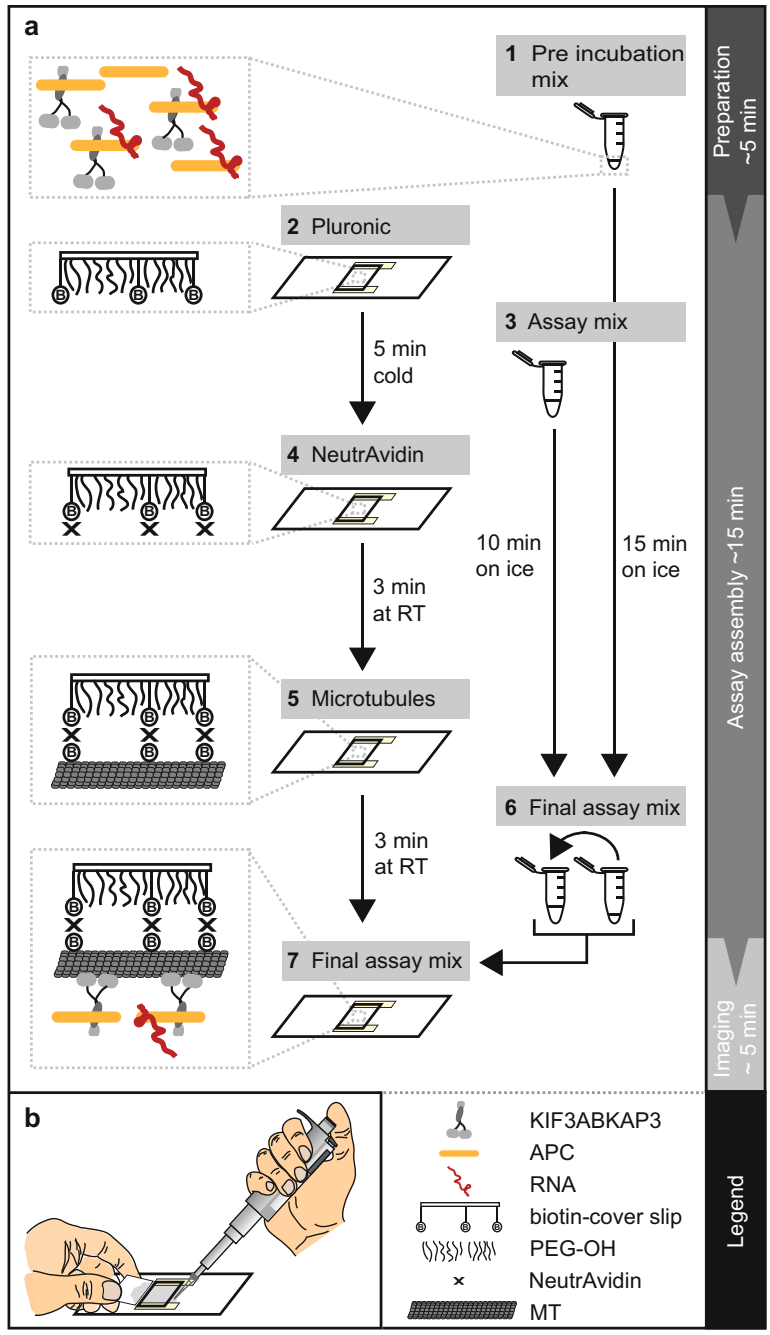

Fig. 2 TIRF-M experiment preparation. (**a**) Schematic representation of the successive steps required for TIRF-M experiment preparation. Steps are performed according to the indicated numbering. The right column (steps 1, 3, and 6) includes steps carried out in tubes on ice. The central column (steps 2, 4, 5, and 7) corresponds to steps in which different solutions are flown through microscopy chambers. Times noted next to arrows correspond to incubation times between individual steps, whereas the gray timeline on the right side corresponds to actual working time including all pipetting steps. The left column visualizes the outcome of every step, from assembly of transport complexes in solution (top) to reconstitution of full transport complexes on microtubules tethered to biotinylated coverslips (bottom). For more information, *see* Subheading 3.3. (**b**) Schematic representation of the handling of microscopy chambers. Individual solutions are pipetted next to microscopy chambers and flown through the latter with the help of small pieces of Whatman™ paper

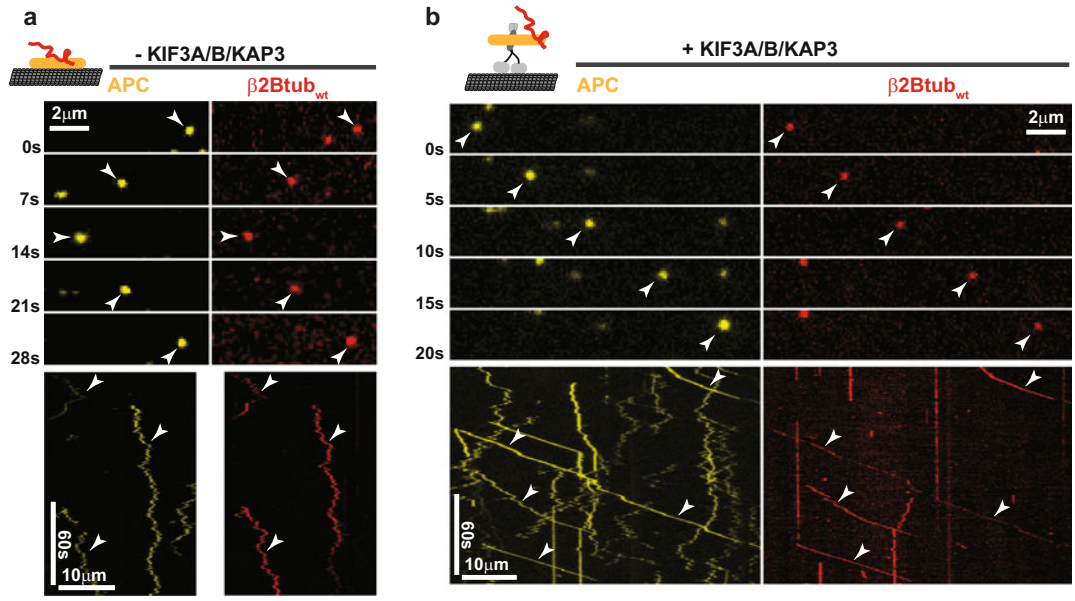

Fig. 3 In vitro reconstitution of axonal mRNA transport. (**a**) Still image series and kymographs of reconstituted APC-TMR (40 pM) and β2Btub-RNA-Alexa647 (2 nM) complexes diffusing on immobilized paclitaxel-stabilized microtubules. (**b**) Still image series and kymographs of reconstituted APC-TMR (80 pM), β2Btub-RNA-Alexa647 (2 nM), and KIF3ABKAP3 (750 pM) complexes showing both diffusive and processive movement on paclitaxel-stabilized microtubules

pM-range concentrations, it can bind one β2B-tubulin RNA per monomer. This stoichiometry and the fact that one kinesin-2 mostly carries one APC dimer lead to the observation that reconstituted mRNA transport complexes mostly carry two RNAs at saturating RNA concentrations. Interestingly, subtle variants of G-rich motifs found in β-actin and β2B-tubulin mRNAs are sufficient to fine-tune the affinity of different RNAs to the transport complex, which leads to a strong preference of β2B-tubulin mRNA transport over β-actin mRNA transport at equal concentrations.

In this chapter, we provide a detailed protocol on the reconstitution of a kinesin-based mRNA transport complex and highlight critical steps and considerations.

2 Materials

2.1 Buffers

1. 2× assay buffer stock (2× AB stock): 180 mM HEPES (Sigma #H3375), 20 mM PIPES (Sigma #P6757), 5 mM $MgCl_2$ (Sigma #M2670), 1.5 mM EGTA (Sigma #03777) in purified water (Sigma #W4502), adjusted with KOH (Sigma #P1767) to pH 6.92–6.95 (*see* **Note 1**).
2. BRB80: 80 mM PIPES, 1 mM $MgCl_2$, 1 mM EGTA, adjust with KOH to pH 6.85 with purified water (Sigma #W4502).

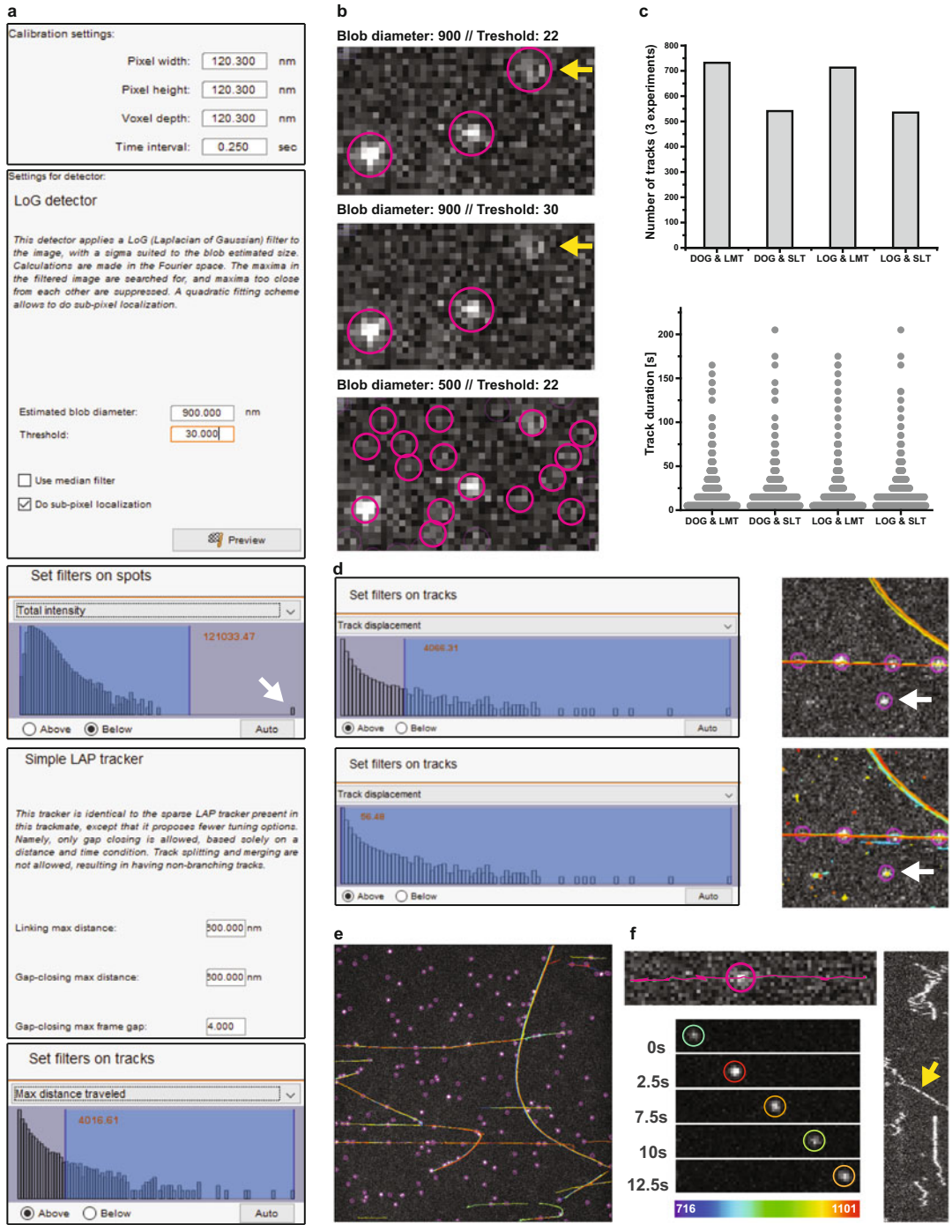

Fig. 4 Automated tracking of mRNA transport complexes. (**a**) Screenshots of Trackmate dialog boxes for important steps. The white arrow indicates an exceptionally bright spot excluded from the analysis by the chosen spot intensity cut-off. (**b**) Examples of points recognized by Trackmate depending on spot diameter and threshold settings. Magenta circles mark recognized spots at this specific time point. The yellow arrow indicates a spot that is recognized at a threshold of 22 but not at a slightly higher threshold of 30. (**c**) Comparison of number of tracks and their duration depending on detector and tracking algorithm chosen. DOG and LOG are different spot detection routines chosen to recognize fluorescent signals (*see* (**a**)). LMT and SLT

3. Filter buffers with 0.2 μm bottle top filter (Merck #S2GPU02RE) and keep in fridge for maximally 3–4 weeks (*see* **Note 2**).

2.2 Microscopy Chambers

1. Object slides (Marienfeld #101200).
2. Double-sided tape (Tesa® #05338).
3. Diamond scriber (MONOCOMP #AGT 5481-A60).
4. Tweezers (Electron Microscopy Science #78322-7(EMS 7)).
5. PLL(20)-g[3.5]-PEG(2) (SuSos AG, Duebendorf, Switzerland) in PBS (2 mg/ml).
6. 1 M NaOH solution.
7. Cover slips functionalized with PEG and Biotin-PEG (Microsurfaces Inc., USA, #Bio_01(2007134-01)).
8. 37 °C incubator.
9. Squeeze bottle with MilliQ water.
10. 100% ethanol (VWR #20821.296).
11. Kimwipes™ (Kimtech Scientific #KIMB7552).

2.3 Microtubule Polymerization

1. 180–230 μM depolymerized tubulin in BRB80 (*see* **Note 3**).
2. 180–230 μM depolymerized and biotinylated tubulin (*see* **Notes 3** and **4**) in BRB80.
3. 180–230 μM depolymerized tubulin labeled with ATTO390 (*see* **Notes 3** and **4**) in BRB80.
4. 100 mM GTP (Sigma #G8877) solution.
5. BRB80 (*see* Subheading 2.1).
6. 37 °C shaker.
7. Paclitaxel (Sigma #T7191).
8. Table centrifuge for 1.5-ml reaction tubes.

Fig. 4 (continued) refer to different tracking algorithms (*see* (**a**)). (**d**) Examples of detected tracks depending on "track displacement" cut-off. (Left) Screenshots of Trackmate with two different cut-offs. (Right) A section of a TIRF-M image with fluorescently labeled β2B-tubulin RNA transported along microtubules with the cut-offs shown in the left panel. Magenta circles mark recognized spots at this specific time point. Colored lines and dots indicate detected tracks over the whole duration of the movie. The white arrows indicate a static event that is only detected with the low track displacement cut-off. Note that in the upper panel the spot is recognized (magenta circle), but only in the lower panel, the track is marked in yellow to indicate a tracked event. (**e**) Whole frame (512 × 512 pixels) of a tracked movie at a specific time point. With the cut-off chosen, only tracks with a displacement above 4 μm are displayed. (**f**) Track example displayed as Trackmate track (upper left panel) and kymograph (right panel, yellow arrow). The lower left panel shows different time points of the respective track, exhibiting different intensities that are indicated by differently colored circles. The heatmap with numbers at the bottom indicates fluorescence arbitrary units

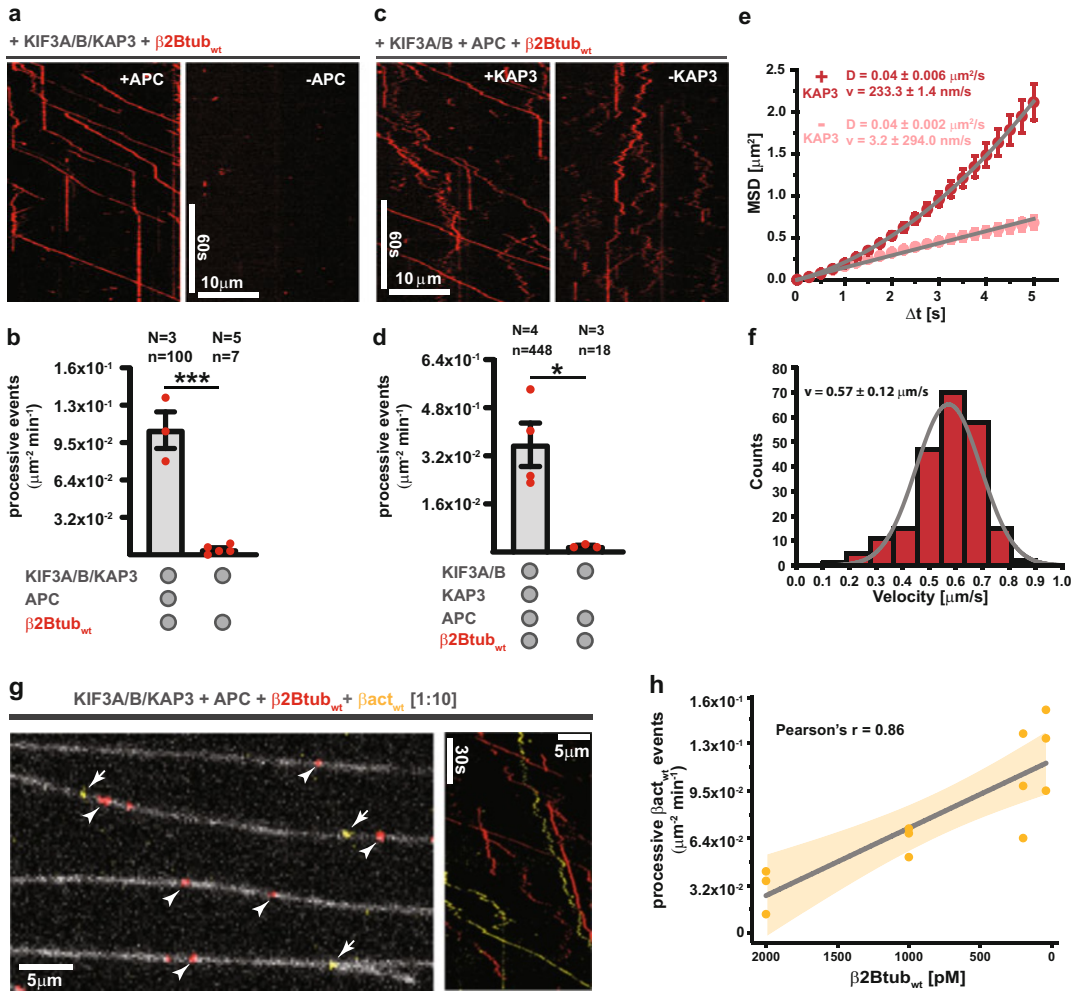

Fig. 5 Analysis of reconstituted mRNA transport complexes. (**a**) The kymographs show Alexa647-β2Btub$_{wt}$—RNA signals from TIRF-M experiments with (left) or without (right) APC. (**b**) Quantification of processive β2Btub$_{wt}$ run events in the presence and absence of APC. N: number of independent experiments, n: total number of events. Error bars: SEM. Statistical significance was evaluated with an unpaired, two-tailed *t*-test. ***$p < 0.001$. (**c**) The kymographs show Alexa647-β2Btub$_{wt}$ signals from TIRF-M experiments containing 750 pM KIF3AB, 150 pM APC, 2 nM Alexa647-β2Btub$_{wt}$, and 500 pM KAP3 (left) or no KAP3 (right). (**d**) Quantification of processive Alexa647-β2Btub$_{wt}$ run events in the presence and absence of KAP3. Error bars: SEM. Statistical significance was evaluated with an unpaired, two-tailed *t*-test. **$p < 0.01$, *$p < 0.05$. N: number of independent experiments, n: total number of events. (**e**) MSD plots of Alexa647-β2Btub$_{wt}$ motility (displacement >1.1 μm to include non-processive events in experiments lacking KAP3) from experiments shown in (**c**). (**f**) Mean instantaneous velocity distribution of processive (displacement >4 μm) Alexa647-β2Btub$_{wt}$ complexes. Gray line: A gauss fit to velocity distribution. (**g**) An overview TIRF-M image (left) and kymograph (right) showing Alexa647-β2Btub$_{wt}$ and TMR-β-actin$_{wt}$-RNA transport in the same experiments at 1:10 molar ratio (200 pM:2 nM). Arrows and arrowheads point to TMR-β-actin$_{wt}$ and Alexa647-β2Btub$_{wt}$ RNPs, respectively. (**h**) A titration of Alexa647-β2Btub$_{wt}$ from 2000 to 40 pM leads to an increase of the relative amount of TMR-β2Btub$_{wt}$ transport per experiment

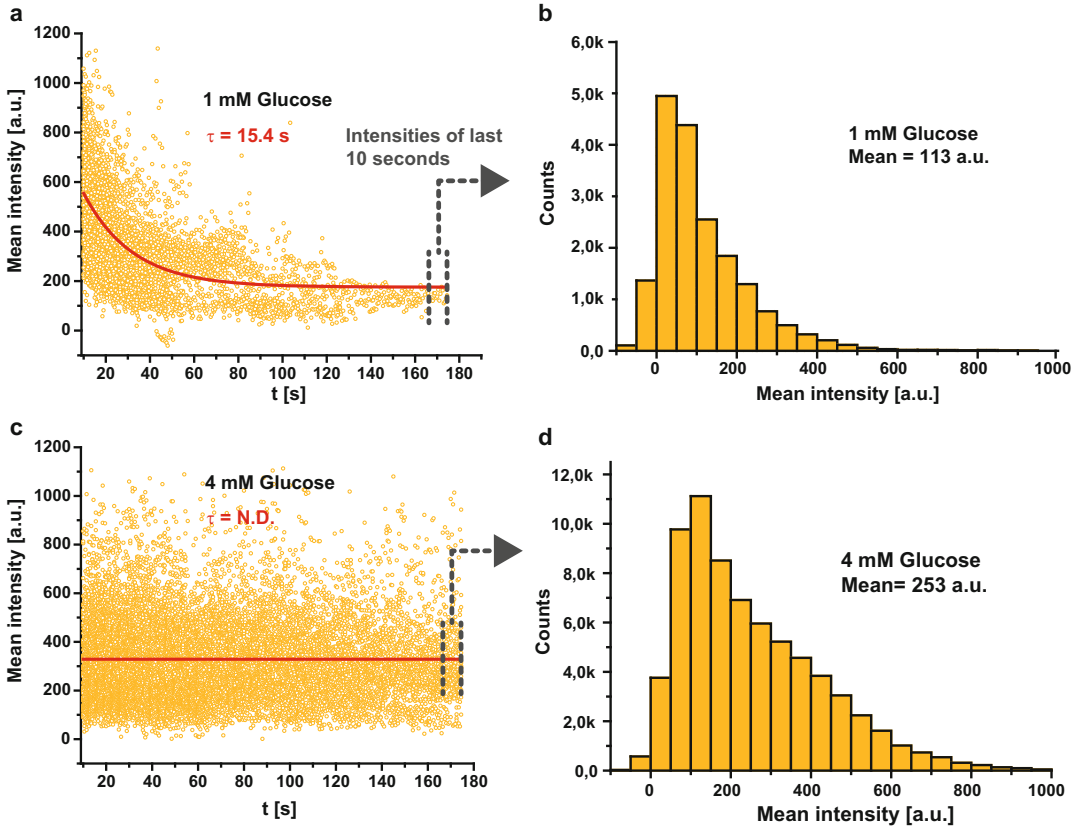

Fig. 6 Important considerations for single-molecule quantifications: bleaching conditions. (**a**) Mean spot intensities over time from a bleaching experiment of KIF3A-TMR immobilized on paclitaxel-stabilized microtubules with AMPPNP are shown. The concentration of glucose was lowered from 50 to 1 mM. (**b**) The distribution of mean spot intensities in the last 10 s of the bleaching experiment shown in (**a**). (**c**) Same experiment as in (**a**) but the concentration of glucose was only lowered from 4 mM. (**d**) The distribution of mean spot intensities in the last 10 s of the bleaching experiment shown in (**c**)

2.4 Oxygen Scavenger and Blocking Reagents

1. For each day of microscopy, prepare solutions of glucose oxidase (AMSBIO #22778.02, 20 mg/ml), catalase (Sigma #C40, 6 mg/ml), β-casein (Sigma #C6905, 5 mg/ml), and κ-casein (Sigma #C0406, 5 mg/ml) in BRB80 (*see* Subheading 2.1).
2. Spin at 80,000 rpm in tabletop ultracentrifuge and TLA120.2 rotor (Beckman Coulter) for 15 min at 4 °C and transfer supernatant (SN) into fresh 1.5-ml reaction tube (*see* **Note 5**).

2.5 TIRF Microscopy

1. iMIC (TILL Photonics, Germany) total internal reflection fluorescence (TIRF) microscope equipped with:
   (a) Three Evolve 512 EMCCD cameras (Photometrics, UK).
   (b) 100 × 1.49 NA objective lens (Olympus, Japan).
   (c) Quadband filter (405/488/561/647, Semrock, USA).

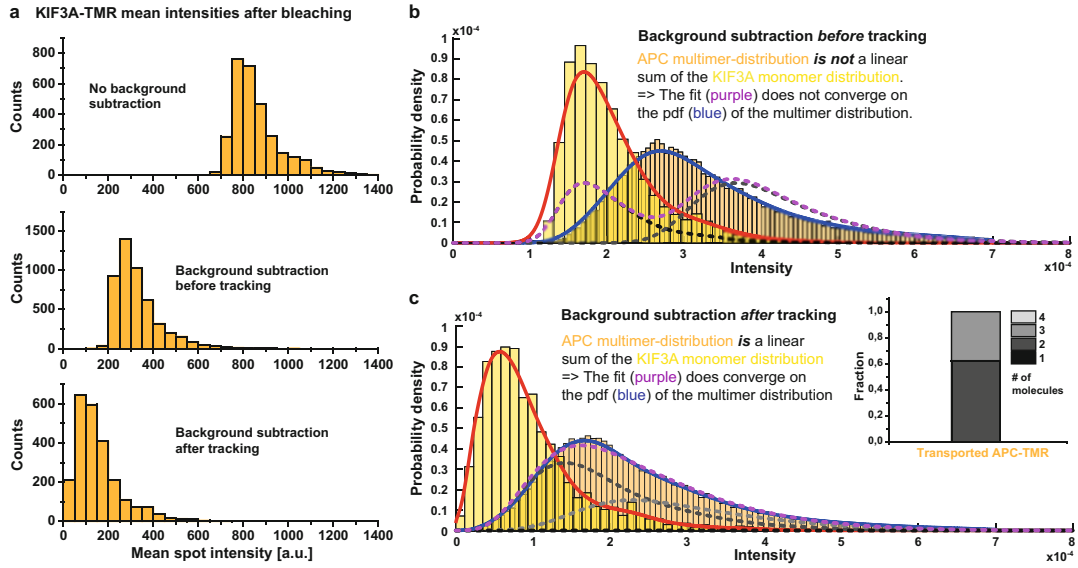

Fig. 7 Important considerations for single-molecule quantifications: background subtraction. (**a**) Mean intensity distribution of immobilized KIF3A-TMR complexes from the last 10 frames of a bleaching experiment. Upper panel: mean intensity distribution without background subtraction. Middle panel: mean intensity distribution of the same data shown in the upper panel but with intensities subtracted before tracking using the ImageJ background subtraction tool (Process > Subtract background). Lower panel: Mean intensity distribution of the same data as show in the upper panel but with background intensities subtracted manually after tracking. (**b**) Attempt to fit linear combinations of the monomeric KIF3A-TMR intensity distribution (bright yellow) obtained from data with background subtraction before tracking to intensity distribution of transported APC-TMR complexes (dark yellow). The fit (purple) does not converge on the pdf of the multimeric distribution (blue). (**c**) Fit of linear combinations of the monomeric KIF3A-TMR intensity distribution obtained from data with background subtraction after tracking to APC-TMR intensity distribution as shown in (**b**). The fit (purple) converges on the pdf of the multimeric distribution (blue). Analysis of the fraction of underlying x-meric distributions reveals that on average two to three APC monomers are transported (inset)

(d) Four different laser lines (405 nm, 488 nm, 561 nm, 639 nm).

(e) Olympus tube lens adds a post magnification of 1.33×, which results in a nominal final pixel size of 120.3 nm.

2. Pipettes 2 × 200 µl, 2 × 20 µl, 1 × 10 µl, 1 × 2.5 µl.
3. Two styrofoam boxes with lids.
4. Microscopy chamber prepared with 100 µm TetraSpeck beads (Invitrogen #T-7279).
5. Whatman™ paper (GE Healthcare #3030-917).
6. Filter tips for 10, 20, and 200 µl.
7. Aluminum blocks for reaction tubes.
8. Aluminum block for chamber on ice.
9. Aluminum block for chamber at RT.

10. NeutrAvidin (Invitrogen #A-2666) in PBS + 20% glycerol (5 mg/ml); 5 µl aliquots in PCR tubes stored at −80 °C or liquid nitrogen.
11. 10% Pluronic F-127 (Sigma #P2443) in MilliQ water.
12. 2% Methylcellulose (Sigma #M0512) in MilliQ water.
13. RNase inhibitor (Invitrogen #AM2694).
14. PEG-3350 (Sigma #1546547-1G).
15. 100 mM ATP (Sigma #A2383) solution in MilliQ water adjusted with KOH to pH 7.15.
16. β-Mercaptoethanol (Sigma #M3148).
17. 1110 mM Glucose (Sigma #G7021) solution in MilliQ water.
18. RNase-free water (ThermoFisher #AM9937).
19. 0.5-ml LoBind reaction tubes (Eppendorf #0030 108.094).
20. 1.5-ml LoBind reaction tubes (Eppendorf #0030 108.116).
21. PCR tubes (Brandt #BR78130).

2.6 Software

1. Tracking with ImageJ and Trackmate:
   (a) Fiji (ImageJ 1.52n) with Trackmate [26] and Multiple Kymograph plugins.
   (b) GraphPad Prism or Origin to plot and statistically test obtained data.
2. Analysis of mRNA transport dynamics:
   (a) GraphPad Prism or OriginLab to plot and statistically test obtained data.
   (b) MATLAB with the MSD analyzer toolbox [28] installed.

2.7 Fluorophore Intensity Calibration and Stoichiometry Measurements

1. AppNHp (AMPPNP) (Jena Bioscience #NU-407-10).
2. For all other materials refer to Subheading 2.5.

3 Methods

3.1 Microscopy Chambers

1. Two days before imaging, place object slides into glass hybridization chambers and add 1 M NaOH (Fig. 1(1)) (*see* **Note 6**).
2. Next day, wash the slides, without removing them from the chamber, three times with purified or MilliQ water (Fig. 1(1)) and discard water.
3. After adding 100% ethanol (Fig. 1(1)) into the chamber, remove slides one by one with thumb and index finger, blot

excess ethanol at the opposite (Fig. 1(2)), downward facing short edge on a tissue, quickly wipe clean with two Kimwipes™ (folded three times) on both sides (*see* **Notes 7** and **8**) and remove residual ethanol with a fresh Kimwipe™.

4. Place clean slides into object slide box to protect them from dust.
5. Cut two strips of double-sided Tesa® tape for each object slide and attach them to the edge of the laboratory bench until further use. Handle Tesa® strips with forceps.
6. Transfer two strips to each slide and position them in parallel and aligned (*see* **Note 9**) (Fig. 1(3)).
7. Pipette 4 µl PLL-PEG between the Tesa® strips with a 20-µl pipette and distribute it between the strips with the pipette tip (Fig. 1(4)).
8. Leave the slides on the bench and let PLL-PEG dry for 15 min at RT.
9. Rinse excess PLL-PEG with MilliQ water from a squeeze bottle (Fig. 1(5)) (*see* **Note 10**). Handle each slide one by one.
10. Remove excess water from the backside of each slide with a Kimwipe™ and shake off excess water with a swift move of your wrist (Fig. 1(6)). Place slides in slide box and transfer to 37 °C incubator for 20–25 min (Fig. 1(7)) (*see* **Note 11**).
11. Transfer slides into new slide box and check if each slide is dry. If not, remove residual water at edges with a Kimwipe™.
12. Cut biotinylated coverslips with a diamond cutter into four equal pieces by placing the coverslip onto an EtOH-cleaned object slide with the biotinylated side facing upward and the mark (*see* **Note 12**) in the upper left corner. Use another EtOH-cleaned object slide as a ruler and place it with one of the long edges centrally onto the coverslip. Cut with diamond cutter to obtain two equal halves. Repeat procedure with the halves to result in equal quarters (Fig. 1(8a)).
13. Remove protective layer from Tesa® strips (Fig. 1(8b)) and attach one coverslip piece to each object slide with the biotinylated surface facing the inside of the chamber. Align on one side with the Tesa® strips. Press down the coverslip gently in parts overlapping with the Tesa® strips with the backside of the tweezers (Fig. 1(9)).
14. Place slides for each experimental day in a separate box (Fig. 1(10)). Put the box into sealable plastic bag containing silica bags and store at 4 °C until 30 min before imaging session. Open the bag only after reaching RT.

3.2 Microtubule Polymerization

1. To obtain microtubules with stochastically incorporated labeled tubulin, mix together depolymerized tubulin (f.c. 30 μM), depolymerized and biotinylated tubulin (f.c. 10 μM), depolymerized and fluorescently labeled tubulin (f.c. 14 μM) as well as GTP (f.c. 4 mM) in BRB80 resulting in 25 μl total volume (*see* **Notes 13** and **14**).
2. Mix by pipetting slowly up and down and incubate at 37 °C in shaker at the lowest revolution (300 rpm) for 25 min.
3. Add 175 μl of prewarmed BRB80 containing 20 μM paclitaxel (*see* **Note 15**), pipette 2–3 times slowly up and down and incubate for 60 min at 37 °C in shaker at 300 rpm.
4. Pellet polymerized microtubules for 5 min at >16,000 × *g*. Remove SN and dissolve MTs in 30 μl BRB80 with 20 μM paclitaxel by pipetting slowly up and down until solution is homogenous (*see* **Note 16**).
5. Store MTs at RT protected from light until further use (*see* **Note 17**).

3.3 TIRF Microscopy

To make sure the overall experiment setup time does not vary between replicates, we recommend using a separate timer to record the time from thawing of reagents until imaging starts. This is especially important for sensitive proteins that might lose their activity over time after thawing.

1. On the day of microscopy, store proteins in a Dewar vessel filled with liquid nitrogen and place the latter next to the microscope.
2. Switch on the microscope, align lasers if necessary and take a reference movie with the chamber containing TetraSpeck beads.
3. Supplement 10 ml of 2× AB stock with 30 mM β-mercaptoethanol and 8 μM paclitaxel to obtain 2× AB.
   (a) Mix 480 μl 2× AB with 500 ul Pluronic and 20 μl κ-casein to obtain pluronic block buffer.
   (b) Supplement 2× AB with 8% PEG-3350 to obtain the final assay buffer 2× AB^{RNArun}.
4. Mix 5 ml of 2× AB with 5 ml RNase-free water to obtain 10 ml 1× AB.
5. Mix 5 ml 1× AB with 50 μl κ-Casein. 110 μl of 1× AB with κ-casein is mixed with 0.8 μl NeutrAvidin to obtain 110.8 μl NeutrAvidin buffer. This amount covers two consecutive experiments (*see* **Note 18**).
6. In total, tubes per day of imaging should be prepared with (*see* **Note 19**):

(a) Pluronic block buffer.
(b) 2× AB^{RNArun}.
(c) RNase-free water.
(d) Glucose (*see* **Note 20**).
(e) Methylcellulose.
(f) Glucose oxidase.
(g) Catalase.
(h) β-Casein.
(i) 1× AB.
(j) NeutrAvidin buffer.
(k) ATP (*see* **Note 21**).
(l) RNase inhibitor (*see* **Note 22**).

7. And additional tubes for each experiment:
   (a) Tube for preincubation mix (0.5-ml tube).
   (b) Tube for final assay mix (0.5-ml tube).
   (c) Tube for protein/RNA dilutions (0.5-ml tube).
   (d) Tube with 45–50 μl 1× AB for MT dilution at RT.
   (e) Tube with 110.8 μl NeutrAvidin buffer for two experiments.
8. Place all tubes in aluminum blocks on ice in a box (*see* **Note 23**).
9. Prepare a second box with ice, place a PCR aluminum block upside down onto the ice and add a piece of Parafilm, bigger than an object slide, on top of it (*see* **Note 24**).
10. Prepare the preincubation mix with 2× AB^{RNArun} (1× f.c.), RNase-free water, 2.5 mM ATP, and 0.5 U RNase inhibitor in a total volume of 10 μl (Fig. 2(1)). Mix properly and leave until further use.
11. Thaw RNA and proteins, dilute after thawing if necessary, and add immediately to preincubation mix (Fig. 2(1)) (*see* **Notes 25** and **26**). Mix quickly but gently by pipetting up and down 15× with a 10 μl pipette and incubate on ice (*see* **Notes 27** and **28**).
12. Take out a chamber from the slide box in the plastic bag, place it at RT and seal bag with the remaining slides. Take a 200 μl pipette, set to 100 μl and fill with Pluronic block buffer. Place the chamber now on the ice block and immediately flow Pluronic block buffer through the chamber (Fig. 2(2)) (*see* **Note 29**).
13. Fill assay mix tube with 2× AB^{RNArun} (1× f.c.), RNase-free water (mix 20×), glucose (50 mM f.c.), methylcellulose

(0.123% f.c.), and mix 20× with the second 200 µl pipette set to 50 µl (Fig. 2(3)) (*see* **Note 30**).

14. Add glucose oxidase (0.32 µg/ml f.c.), catalase (0.275 µg/ml f.c.), β-casein (50 µg/ml f.c.) and mix gently by pipetting up and down 20× with a 20 µl tip (Fig. 2(3)) (*see* **Note 31**).
15. After 5 min 30 s (timer counting down) of Pluronic incubation of the chamber, prepare one 200 µl pipette with 1× AB and set aside. Prepare the second 200 µl pipette with 50 µl NeutrAvidin buffer and flow it quickly through chamber. Immediately after, flow 1× AB and place on chamber on aluminum block at RT (*see* **Note 32**) (Fig. 2(4)). The incubation time of this step is 3 min.
16. After 2 min (1 min 20 s on the timer counting down), start preparing MT dilution by adding 3–6 µl of MT stock (*see* Subheading 3.2) to 1× AB to reach a final volume of 50 µl and mix gently 5×. As soon as the timer counting down beeps, flow MT dilution into chamber (Fig. 2(5)). Set timer again to count down from 3 min.
17. Add ATP (2.5 mM f.c.) to the assay mix and pipette 10× up and down with 20 µl tip.
18. After 2 min 30 s (timer counting down) of MT incubation at RT, add preincubation mix to the assay mix (Fig. 2(6)) to obtain the desired final protein and RNA concentrations in the final assay mix. As soon as the timer counting down is completed, mix the final assay mix by pipetting 10× with 200 µl pipette set to 59 µl and flow 59 µl of final assay mix through chamber (Fig. 2(7)) (*see* **Note 33**).

    Seal chamber with nail polish and begin imaging immediately (*see* **Note 34**).

3.4 Tracking with ImageJ and Trackmate

1. Load movie stack into Fiji.
2. Calibration settings: Enter pixel size and frame rate (Fig. 4a). This can also be set globally under the Fiji menu item "Image > properties" and will then apply to all movies loaded as long as Fiji is not closed.
3. Choose LoG or DoG Detector (Fig. 4a). We tested LoG and DoG detectors for our data which produced similar results (Fig. 4c).
4. Enter blob diameter and threshold: Make sure not to cut off pixels belonging to a spot if, e.g., total or mean intensities are of interest for later analysis (Fig. 4a, b) (*see* **Note 35**).
5. Hit "Preview" and use Fiji's contrast functions to manually validate that detected spots are correct. Inspect different time points to the movie in case intensities change over time.

6. Set filter on spots: After spot detection one can exclude spots (Fig. 4a) (*see* **Note 36**).
7. Choose tracker: Both the Simple Lap Tracker (SLT) and Linear Motion Tracker (LMT) worked well for our samples. The LMT found more but slightly shorter tracks (Fig. 4a, c).
8. Choose tracker tuning options that do not cause artifacts, e.g., by splitting tracks due to intensity fluctuations or link tracks that belong to different events. Also *see* **step 10** below.
9. Set filter on tracks: Setting a displacement cut-off is ideal, e.g., to include or exclude diffusive events once their characteristic displacement has been determined. We always set a minimal "track displacement" (*see* **Note 37**) cut-off of >1.1 μm to exclude molecules that stick unspecifically to the coverslip (Fig. 1d) (*see* **Notes 38** and **39**).
10. Manual control: Create kymographs along detect tracks, e.g., using Fiji's reslice option "Image > Stacks > Reslice." Check if tracks detected by Trackmate reflect number and duration of actual events. If not, adjust detector and tracking settings.
11. Export data: Hit "Analysis" button. Save tracks and spots tables for subsequent analysis of motility and intensity parameters. While the "track" files contain dynamic information, the "spot" files contain intensity information.

3.5 Analysis of mRNA Transport Dynamics

The track tables produced by Trackmate can directly be used for straightforward analysis such as determining the number of processive run events (Fig. 5a–d) or the mean velocity distribution among processive events (Fig. 5e). Importing of track files into analysis tools as MSD analyzer (MATLAB) allows computing of mean square displacement curves (Fig. 5f). For experiments with two differently labeled RNAs (Fig. 5g) in the same experiment (β2Btub$_{wt}$-Alexa647 and βact$_{wt}$-TMR), both channels can be tracked independently to later join data for comparative analysis, e.g., using OriginLab (Fig. 5h).

3.6 Fluorophore Intensity Calibration and Stoichiometry Measurements

To dissect the stoichiometry of reconstituted mRNA complexes and sub-complexes, we first determined the intensities of individual TMR and Alexa647 fluorophores coupled to a dimeric KIF3A-SNAP construct. To image these calibration probes under conditions as close to the actual transport complexes as possible, we immobilized labeled KIF3A calibration probes on paclitaxel-stabilized microtubules inside TIRF-M chambers using the ATP analog AMPPNP. While illumination settings can be kept very stable for several days depending on the microscope set up used, it is highly recommended to image both the calibration probe and the sample to be analyzed on the same day using the same imaging settings. To determine the average number of molecules in

transport complexes, we fitted linear combinations [27, 29] of the predetermined monomeric (and the resulting multimeric) fluorophore intensity distributions to the intensity distributions obtained from tracking the kinesin, APC, and RNAs.

We would like to highlight two important considerations (1). To make sure that one records single fluorophores as a calibration probe, bleaching conditions have to be properly established. We found that it requires lowering of the glucose in the TIRF-M imaging buffer from 50 to 1 mM in order to obtain image information with mostly single-fluorophores per spot in a reasonable time (Fig. 6). Once the intensities in a bleaching curve reach a stable minimum with little variation (Fig. 6a, b), one can assume that such a condition is found. Little difference in the glucose concentration can have a large effect; when using 4 mM instead of 1 mM glucose, no considerable bleaching was detected withing 3 min of imaging (Fig. 6c, d) (2). Another important aspect is how and when the image background is subtracted. We tested subtracting the background before tracking using tools included in Fiji (Process > Subtract background) and measuring the background manually [27] and subtracting it using Fiji (Process > Math > Subtract). Alternatively, we subtracted the manually measured mean background directly from the spot mean intensity values produced by Trackmate. The mean background was manually measured by averaging the mean intensity in a rectangular box at five positions of the field of view in four frames over the entire movie. This resulted in different mean intensity distributions for our KIF3A calibration samples. An example of intensity distributions obtained from immobilized KIF3A-TMR is shown in Fig. 7a. There is a notable difference in the distributions obtained when subtracting the background before and after tracking. The reason for this is that both background subtraction methods before tracking artificially increase mean spot intensities, as pixels in Fiji cannot have negative values after the "Subtract" or "Subtract background" procedure. However, there are pixels within a spot recorded by Trackmate that would have negative intensity values after mean background subtraction. When subtracting a manually measured mean background value from the spot intensity value, this problem does not occur. As a result, multimeric intensity distributions, as e.g., derived from tracking APC-TMR transported by KIF3AB-KAP3, can be fitted to linear combinations of the predetermined KIF3A-TMR intensity distribution to obtain the number of molecules in a complex (Fig. 7b, c).

1. Follow steps in Subheading 3.3.
2. Instead of using ATP, use 2.5 mM AMPPNP (f.c.).
3. Instead of using 50 mM glucose (f.c.), use 1 mM glucose (f.c.).

4. Image with the exact same settings used in the actual experiments.
5. Track TIRF-M movies with Trackmate using the same tracking parameters as before. It is important to include only tracks lasting longer than 3 s, to make sure one does not include transient, unspecifically binding molecules that have not been bleached.
6. Confirm that obtained mean spot intensities reach a stable minimum at the end of the recorded movie (Fig. 6a).
7. Use the mean spot intensity distribution from the last 10 frames of the movie as monomer fluorescence intensity calibration data set.

4 Notes

1. To keep the ionic strength of the buffer constant, it is recommended to use 1.21 g of KOH per 250 ml of buffer and confirm the correct pH, which may slightly differ with changing RT.
2. Use bottle top filters with plastic bottles to ensure buffers are free of contaminants that might originate from reused glassware.
3. The concentrations of depolymerized tubulin, depolymerized, and biotinylated tubulin as well as depolymerized and fluorescently labeled tubulin may vary. Our stock solutions commonly have concentrations around 185 μM, 184 μM, and 99 μM, respectively.
4. Tubulin is labeled according to published protocols [30].
5. If prepared for 2 days of microscopy, split in two tubes, and keep half in box with ice and place in cold room or refrigerator.
6. In general, one can prepare around eight chambers per day of microscopy. One experiment including preparation and imaging time takes about 40–45 min. After eight experiments, the buffer performance might decrease.
7. It is recommendable to clean nitril gloves with soap beforehand to prevent any dust contaminations coming from the gloves.
8. Check slides against light for any visible contaminations. In case you detect streaks or smears by eye repeat EtOH step.
9. Make sure the Tesa® strips have no dents or kinks. Turn around object slides and check if Tesa® strips are properly attached.
10. Usually one needs ~300–400 ml H_2O per six slides.
11. The incubation time increases with the amount of slides per box.

12. Commercial biotin-slips from Microsurfaces are marked at one corner.
13. The final concentration of depolymerized and biotinylated tubulin as well as depolymerized and fluorescently labeled tubulin may vary according to the labeling ratio and brightness of the fluorophore. When using ATTO390 at a labeling ratio of ~20%, the here mentioned concentrations will result in sufficient signal.
14. Depending on the desired MT density on the biotinylated coverslip and days of microscopy, the volume needs to be adjusted.
15. Keep BRB80 with paclitaxel at 37 °C and vortex extensively before adding.
16. The pellet with ATTO390-labeled microtubules appears white.
17. The best results are obtained when MTs are prepared on the day of microscopy; however, they are relatively stable for up to 2 days. This also depends on the fluorophore used.
18. Add NeutrAvidin immediately before the first of two experiments.
19. All solutions are prepared in 1.5-ml tubes unless otherwise stated.
20. Prepare 50 µl aliquots for each day of imaging in PCR tube.
21. Prepare 25 µl aliquots for each day of imaging in PCR tube.
22. Prepare a PCR tube with 2 µl per four experiments immediately before imaging. After four experiments, prepare a fresh PCR tube.
23. Styrofoam boxes with lids are convenient to prevent melting of ice and excess condensation on metal blocks. This helps keeping contaminations to a minimum.
24. The Parafilm helps removing the object slide from the block when transferred later to an aluminum block at RT.
25. Take 2–3 µl aliquot of RNA out of freezer immediately before adding to preincubation mix. Thaw RNA quickly and add first to the preincubation mix.
26. Take a PCR tube containing protein solution from liquid nitrogen and place on ice. Open tube quickly and close to prevent potential bursting of the tube. Typical protein concentrations in the preincubation mix are in the lower nanomolar range (5–50 nM). RNA concentrations range from 10 to 280 nM. The resulting concentrations within the final assay mix (*see* **step 18**) for proteins and RNAs are in the low to mid picomolar and low nanomolar range for proteins and RNA, respectively.

27. Pipetting too rapidly and excessively may denature proteins due to the air–liquid interfaces created at foam bubbles.
28. Fifteen times because the solution is viscous due to PEG-3350 and methylcellulose.
29. Be quick so that humidity cannot condense before Pluronic enters the chamber. The flow speed is comparably slow because of viscosity. To increase flow speed, change position of Whatman™ paper slightly sideways and/or lift the Whatman™ paper a tiny bit and place it on top of the first <1 mm of the coverslip. Note that at other steps such as flowing in the less viscous NeutrAvidin buffer, the flow speed may be very quick this way. In particular when flowing MTs into the chamber, you may want to keep the speed low, because it increases the amount of MTs attached to the glass.
30. First, buffer and water as well as chemicals dissolved in water are mixed before proteins are added.
31. Because of the viscosity, it is recommendable to use a smaller volume with more repetitions to mix. This way less assay mix sticks to the pipette tip.
32. If you experience a high amount of fluorescent protein or RNA sticking to the coverslip during imaging, try to decrease the amount of NeutrAvidin in the chamber by increasing flow speed or decreasing the amount of NeutrAvidin in the NeutrAvidin buffer. Be aware that less NeutrAvidin can lead to unstably attached MTs.
33. Remove excess final assay mix on both slides of the coverslip with a piece of Whatman™ paper. Be careful not to suck assay mixture out of the imaging chamber.
34. Depending on the stability of proteins and RNAs under the assay condition, it can be crucial to keep the time between chamber sealing and begin imaging as constant as possible.
35. The threshold differs depending on depending on fluorophore and concentration.
36. Usually we exclude spots above a certain intensity threshold, to exclude occasionally appearing aggregates.
37. To exclude diffusive events, either “track displacement” or “maximum distance travelled” is useful when set to >6 μm. The value might differ, depending on the molecules studied, and was experimentally determined in this case. “Max distance travelled” is included in the additional plugin “Track analysis” for Trackmate.
38. The cut-off can be as high as 2 μm, depending on the kind of molecule studied and its motion behavior. Also, it depends on the fluorophore chosen, concentration, and other settings, such as threshold and gap size.

39. Although our approach allows for rapid analysis of motility parameters, landing rates of molecular motors, for instance, can only be addressed by different means, such as manually generating and analyzing kymographs.

Acknowledgments

This work was supported by the Spanish Ministry of Economy and Competitiveness (MINECO) [BFU2017-85361-P], [BFU2014-54278-P], [BFU2015-62550-ERC], by the Juan de la Cierva-Incorporación Program [IJCI-2015-25994], the Human Frontiers in Science Program (HFSP) [RGY0083/2016], the European Research Council (ERC) [H2020-MSCA-IF-2014-659271] and the Ministerio de Ciencia, Innovación y Universidades and Fondo Social Europeo (FSE) [PRE2018-084501]. We further acknowledge support of the Spanish Ministry of Economy and Competitiveness to the EMBL partnership, "Centro de Excelencia Severo Ochoa" [SEV-2012-0208] and [SEV-2015-0533], and the CERCA Programme/Generalitat de Catalunya.
We would further like to thank Stefan Wieser and Verena Ruprecht for the helpful discussions on image analysis.

References

1. Buxbaum AR, Haimovich G, Singer RH (2015) In the right place at the right time: visualizing and understanding mRNA localization. Nat Rev Mol Cell Biol 16:95–109
2. Holt CE, Bullock SL (2009) Subcellular mRNA localization in animal cells and why it matters. Science 326:1212–1216
3. Holt CE, Martin KC, Schuman EM (2019) Local translation in neurons: visualization and function. Nat Struct Mol Biol 26:557–566
4. Litman P, Barg J, Rindzoonski L, Ginzburg I (1993) Subcellular localization of tau mRNA in differentiating neuronal cell culture: implications for neuronal polarity. Neuron 10: 627–638
5. Litman P, Barg J, Ginzburg I (1994) Microtubules are involved in the localization of tau mRNA in primary neuronal cell cultures. Neuron 13:1463–1474
6. Leung K-M, van Horck FPG, Lin AC, Allison R, Standart N, Holt CE (2006) Asymmetrical beta-actin mRNA translation in growth cones mediates attractive turning to netrin-1. Nat Neurosci 9:1247–1256
7. Lin AC, Holt CE (2007) Local translation and directional steering in axons. EMBO J 26: 3729–3736
8. Yoon YJ, Wu B, Buxbaum AR, Das S, Tsai A, English BP, Grimm JB, Lavis LD, Singer RH (2016) Glutamate-induced RNA localization and translation in neurons. Proc Natl Acad Sci U S A 113:E6877–E6886
9. Miller S, Yasuda M, Coats JK, Jones Y, Martone ME, Mayford M (2002) Disruption of dendritic translation of CaMKIIalpha impairs stabilization of synaptic plasticity and memory consolidation. Neuron 36:507–519
10. Turner-Bridger B, Caterino C, Cioni J-M (2020) Molecular mechanisms behind mRNA localization in axons. Open Biol 10:200177
11. Liao YC, Fernandopulle MS, Wang G, Choi H, Hao L, Drerup CM, Patel R, Qamar S, Nixon-Abell J, Shen Y et al (2019) RNA granules hitchhike on lysosomes for long-distance transport, using Annexin A11 as a molecular tether. Cell 179:147–164.e20
12. Hirano M, Muto M, Sakai M, Kondo H, Kobayashi S, Kariwa H, Yoshii K (2017) Dendritic transport of tick-borne flavivirus RNA by neuronal granules affects development of neurological disease. Proc Natl Acad Sci U S A 114:9960–9965
13. Pocock GM, Becker JT, Swanson CM, Ahlquist P, Sherer NM (2016) HIV-1 and

M-PMV RNA nuclear export elements program viral genomes for distinct cytoplasmic trafficking behaviors. PLoS Pathog 12:1–30

14. Dictenberg JB, Swanger SA, Antar LN, Singer RH, Bassell GJ (2008) A direct role for FMRP in activity-dependent dendritic mRNA transport links Filopodial-spine morphogenesis to fragile X syndrome. Dev Cell 14:926–939
15. Mallardo M, Deitinghoff A, Muller J, Goetze B, Macchi P, Peters C, Kiebler MA (2003) Isolation and characterization of Staufen-containing ribonucleoprotein particles from rat brain. Proc Natl Acad Sci 100: 2100–2105
16. Fritzsche R, Karra D, Bennett KL, Ang F, Heraud-Farlow JE, Tolino M, Doyle M, Bauer KE, Thomas S, Planyavsky M et al (2013) Interactome of two diverse RNA granules links mRNA localization to translational repression in neurons. Cell Rep 5:1749–1762
17. Kanai Y, Dohmae N, Hirokawa N (2004) Kinesin transports RNA. Neuron 43:513–525
18. Järvelin AI, Noerenberg M, Davis I, Castello A (2016) The new (dis)order in RNA regulation. Cell Commun Signal 14:9
19. Alberti S, Saha S, Woodruff JB, Franzmann TM, Wang J, Hyman AA (2018) A User's guide for phase separation assays with purified proteins. J Mol Biol 430:4806–4820
20. Tushev G, Glock C, Heumüller M, Biever A, Jovanovic M, Schuman EM (2018) Alternative 3′ UTRs modify the localization, regulatory potential, stability, and plasticity of mRNAs in neuronal compartments. Neuron 98:495–511. e6
21. Zappulo A, van den Bruck D, Ciolli Mattioli C, Franke V, Imami K, McShane E, Moreno-Estelles M, Calviello L, Filipchyk A, Peguero-Sanchez E et al (2017) RNA localization is a key determinant of neurite-enriched proteome. Nat Commun 8:583
22. Heym RG, Zimmermann D, Edelmann FT, Israel L, Ökten Z, Kovar DR, Niessing D (2013) In vitro reconstitution of an mRNA-transport complex reveals mechanisms of assembly and motor activation. J Cell Biol 203:971–984
23. Sladewski TE, Bookwalter CS, Hong M-S, Trybus KM (2013) Single-molecule reconstitution of mRNA transport by a class V myosin. Nat Struct Mol Biol 20:952–957
24. McClintock MA, Dix CI, Johnson CM, McLaughlin SH, Maizels RJ, Hoang HT, Bullock SL (2018) RNA-directed activation of cytoplasmic dynein-1 in reconstituted transport RNPs. Elife 7:e36312. https://doi.org/10.1101/273912
25. Zacharias DA, Violin JD, Newton AC, Tsien RY (2002) Partitioning of lipid-modified monomeric GFPs into membrane microdomains of live cells. Science 296:913–916
26. Tinevez JY, Perry N, Schindelin J, Hoopes GM, Reynolds GD, Laplantine E, Bednarek SY, Shorte SL, Eliceiri KW (2017) TrackMate: an open and extensible platform for single-particle tracking. Methods 115:80–90
27. Baumann S, Komissarov A, Gili M, Ruprecht V, Wieser S, Maurer SP (2020) A reconstituted mammalian APC-kinesin complex selectively transports defined packages of axonal mRNAs. Sci Adv 6:eaaz1588
28. Tarantino N, Tinevez J-Y, Crowell EF, Boisson B, Henriques R, Mhlanga M, Agou F, Israël A, Laplantine E (2014) TNF and IL-1 exhibit distinct ubiquitin requirements for inducing NEMO-IKK supramolecular structures. J Cell Biol 204:231–245
29. Moertelmaier M, Brameshuber M, Linimeier M, Schütz GJ, Stockinger H (2005) Thinning out clusters while conserving stoichiometry of labeling. Appl Phys Lett 87:1–3
30. Hyman A, Drechsel D, Kellogg D, Salser S, Sawin K, Steffen P, Wordeman L, Mitchison T (1991) Preparation of modified tubulins. Methods Enzymol 196:478–485